Mercury atmospheric emission, deposition and isotopic fingerprinting from major coal-fired power plants in Australia: insights from palaeo-environmental analysis from sediment cores

Larissa Schneider[a], Neil L. Rose[b], Lauri Myllyvirta[c], Simon Haberle[a], Anna Lintern[d], Jingjing Yuan[e], Darren Sinclair[f], Cameron Holley[g], Atun Zawadzki[h], Ruoyu Sun[e]

Authors:

[a] **Larissa Schneider, Simon Haberle**
College of Asia and the Pacific. The Australian National University. Coombs Bld. 9, Fellows Rd. 2601 Canberra, ACT. Australia. Orcid.gov/ 0000-0001-5276-2531

[b] **Neil Rose**
Environmental Change Research Centre, Dept of Geography, University College London, Gower Street, London WC1E 6BT, UK

[c] **Lauri Myllyvirta**
Centre for Research on Energy and Clean Air (CREA), Helsinki, Finland

[d] **Anna Lintern**
Department of Civil Engineering, Monash University, 3800, Clayton, Victoria, Australia.

[e] **Jingjing Yuan, Ruoyu Sun,**
Institute of Surface-Earth System Science, School of Earth System Science, Tianjin University, 300072, Tianjin, China

[f] **Darren Sinclair**
Centre for Change Governance, Institute of Governance and Policy Analysis, University of Canberra, Canberra, Australia

[g] **Cameron Holley**
Faculty of Law, University of New South Wales, Sydney, NSW 2052, Australia

[h] **Atun Zawadzki**
Australian Nuclear Science and Technology Organisation (ANSTO), Lucas Heights, NSW, 2234.

Corresponding author: Larissa Schneider. College of Asia and the Pacific. The Australian National University. Coombs Bld. 9, Fellows Rd. 2601 Canberra, ACT. Australia. Phone +61-429088813/

Keywords: CALPUFF, mercury isotope, bag filter, electrostatic precipitator, Minamata Convention.

Abstract: Despite Australia's high reliance on coal for electricity generation, no study has addressed the extent to which mercury (Hg) deposition has increased since the commissioning of coal-fired power plants. We present stratigraphic data from lake sediments in the Hunter Valley (New South Wales) and Latrobe Valley (Victoria), where a significant proportion of Australia's electricity is generated via coal combustion. Mercury deposition in lake sediments increased in the 1970s with the commissioning of coal-fired power plants, by a factor of 2.9-times in sediments of Lake Glenbawn (Hunter Valley) and 14-times in Traralgon Reservoir (Latrobe Valley). Sediments deposited after the commissioning of power plants have distinct Hg isotope compositions, similar to those of combusted coals. Mercury emission, estimated using an atmospheric model (CALPUFF), was higher in the Latrobe Valley than in the Hunter Valley. This is a result of higher Hg concentrations in lignite coal, lax regulation and older pollution-control technologies adopted by power-plants in the Latrobe Valley. Near-source deposition of Hg in Australia is significantly higher than North America and Europe, where better emission controls (e.g. wet flue gas desulfurization) have been in effect for decades. The challenge for Australia in years to come will be to ratify the Minamata Convention and develop better regulation policies to reduce Hg emissions.

■ INTRODUCTION

Mercury (Hg) is a neurotoxic heavy metal found ubiquitously in the atmosphere and on the Earth's surface (Selin, 2009). Mercury has an atmospheric residence time of ~1 yr, allowing it to be globally distributed (Gustin et al., 2015; Selin, 2009) and eventually deposited on terrestrial or water surfaces. As a result, measurements from natural archives such as lake sediments are useful tools to understand anthropogenic inputs of Hg to the atmosphere and consequent deposition in the environment (Biester et al., 2007; Engstrom et al., 2014)

Human activities such as gold mining and biomass/fossil fuel combustion have led to an increase in Hg emissions compared to pre-industrial times (Selin, 2009). Although Hg is commonly present at trace levels in coal (Sun et al., 2016a), the large quantity of coal used in the energy and industrial sectors have made coal combustion the dominant Hg emission source globally. Coal combustion alone is responsible for more than 20% of the estimated global Hg emissions (UNEP, 2019). The main factors affecting Hg emissions and fate in the

environment during coal combustion include the Hg content of the coal, the type and efficiency of control devices used to reduce gaseous and particulate emissions, and the total amount of coal combusted (Dabrowski et al., 2008; Pavlish et al., 2003).

In Australia, coal accounted for 62% of total electricity generated in 2016-2017 (DEE, 2018), with the largest coal-fired power plants located in the Hunter Valley (NSW) and in the Latrobe Valley (VIC) (Schneider et al., 2020). The Upper Hunter Valley has two major power plants (Liddell and Bayswater) fed by bituminous coal (NSW Planning and Environment, 2019) generating 35% of the electricity needs of the state of New South Wales (NSW). In the Latrobe Valley, electricity is produced from the combustion of predominantly brown coal (lignite) and the valley produces approximately 85% of the electricity for the state of Victoria (VIC) (Weller et al., 2011).

Coal-fired power plants in Australia are characterised by ageing facilities and lack modern devices to control pollution emission (Sinclair and Schneider, 2019). By 2030, around half of the 24 coal-fired power plants in Australia will be over 40 years old, with some plants having operated for nearly 60 years (Stock, 2014). The emission control devices used in these power plants are filter bags in NSW, and electrostatic precipitators in VIC, with neither Hg-specific controls nor acid gas control devices in use. This difference in emission control devices has a significant impact on Hg emissions from coal-fired power stations in NSW compared to VIC. The performance of emission control devices varies according to the operational conditions of the power station. However in general, Hg removal efficiency of bag filters is higher (approximately 80% removal) than that of electrostatic precipitators (approximately 20% removal) (Wang et al., 2008).

Mercury stable isotope geochemistry has been used to determine Hg sources and to track the processes and fate of Hg in the environment by utilising the variation of seven Hg stable isotopes (^{196}Hg, ^{198}Hg, ^{199}Hg, ^{200}Hg, ^{201}Hg, ^{202}Hg and ^{204}Hg) (Sun et al., 2016a). These isotopes exhibit both mass-dependent fractionation (MDF) and mass-independent fractionation (MIF) (Jackson and Muir, 2012), revealing valuable information about sources and biogeochemical cycling of Hg (Bergquist and Blum, 2007). Previous Hg isotopic studies show that coal deposits from different regions, coal-forming periods and maturation ranks are characterized by distinct Hg isotope compositions (Sun et al., 2016a), in which MIF are unaltered by coal combustion processes in coal-fired boilers (Sun et al., 2016b, 2014).

Little is known about Hg emissions and accumulation in different environmental compartments in Australia (Dutt et al., 2009; Howard et al., 2017; Nelson, 2007; Nelson et al., 2012; Schneider et al., 2020) and to the best of our knowledge, no Hg isotopic measurements have been published for the Australian environment. Quantitative assessment of Hg sources, deposition and emission from coal-fired plants in Australia is of substantial interest to both environmental scientists and decision-makers. This is particularly the case in Australia where negotiations to ratify the Minamata Convention are still ongoing (Sinclair and Schneider, 2019).

We studied historical variations in Hg concentrations, Hg deposition fluxes and the isotopic composition of Hg in sediment cores from lakes adjacent to coal-fired power plants in the Hunter and Latrobe Valleys. Mercury isotope records and spheroidal carbonaceous particles (SCPs, a component of fly-ash only derived from the high combustion temperature of coal and oil fuels (Rose, 2001), are used to identify the sources and cycling of Hg in lake sediments. Mercury atmospheric deposition was calculated in these two areas using a detailed long-range atmospheric dispersion model — CALPUFF (Scire et al., 2000). Finally, we assessed the efficiency of retrofitting these power plants with bag filters and discuss the implications of regulatory decisions on Hg emissions in these two areas.

■ MATERIALS AND METHODS

This study was undertaken within areas of major coal deposits in Australia that host the largest coal-fired power plants in the country: the Hunter Valley in NSW and the Latrobe Valley in VIC (Figure 1). These two sites are distinct in coal formation, with the Hunter Valley producing bituminous coals from the Permian (about 250 million years old), with varying volatile matter and ash content (NSW Planning and Environment, 2019), and the Latrobe Valley producing lignite brown coal from the Early-Middle Cenozoic (about 15–50 million years old) with high water content (Australia Government Regional Assessment Program, 2019; Nelson, 2007). The coal mined from both sites supply nearby coal-fired power plants. More information is presented in the Supplementary Material. Coal-fired power plants located in both Hunter and Latrobe Valleys and respective coal types are listed in Table 1.

Sediment, soil and coal collection

Lake Glenbawn, Hunter Valley

We selected dams that are proximal to coal-fired power plants in these two valleys to study the temporal trends in Hg deposition and their relationship with the establishment and operations of coal-fired power plants (Figure 1). Lake Glenbawn in NSW (32.0940° S, 150.9891° E, 280 m a.s.l.) is approximately 30 km northwest of Liddell and Bayswater coal-fired power plants (Figure 1). No coal-mining activities exist within the Lake Glenbawn catchment area. The sediment core collection was completed in May 2018 using a gravity corer fitted with a polycarbonate tube that penetrated the sediment 30 m below the water surface. Disturbance of the water-sediment interface was minimal and maximum penetration in the sediment was 32 cm. The sediment core was sliced every 1 cm in the field and stored in Ziplock bags in the Australian National University Palaeoworks Lab cold room at 4º C. More details about sediment collection and regional climate are presented in the Supplementary Material.

In addition, samples representing the two main Hg sources in the catchment (coal and catchment soils) were obtained. Three bituminous coal samples were obtained from Newstan mine, part of the Newcastle coalfield. This mine is part of the five coal fields that make up the Sydney-Gunnedah coal basin, which is the largest resource of bituminous coal in Australia (Pinetown et al., 2008). Coal mined in this mine is used both domestically and for export.

Soil samples were obtained from two sites on the south side of the Lake Glenbawn catchment Samples were collected by digging approximately 30 g of soil from the 2-4 cm depth layer with a stainless-steel trowel to remove the influence of possible top layer contamination. They were stored in Ziploc bags and stored in the same way as the sediment samples.

Traralgon Railway Reservoir, Victoria

Traralgon Railway Reservoir is located in the Traralgon Conservation Reserve (38°12'35.35"S, 146°31'47.32"E, 64 m a.s.l.), in Victoria (Figure 1). Coal-fired power plants located in the Latrobe Valley include Hazelwood Power Station (decommissioned in 2017), Loy Yang Power Stations A & B, Yallourn Power Station and Yallourn Power Station (Table 1, Figure 1). Traralgon Railway Reservoir is located 16 km from Hazelwood, 18 km from Yallourn and 8 km from Loy Yang A & B power stations.

As for Lake Glenbawn, Traralgon Railway Reservoir has no coal-mining activities within its catchment. A sediment core was taken in April 2018 using a piston corer fitted with a polypropylene tube and a 43 cm core was retrieved at 3 m depth from the water surface. The

core was sliced every 1 cm in the field and stored in Ziplock bags in the Palaeoworks Lab cold room at 4º C at the Australian National University. More details on this reservoir and regional climate are provided in Supplementary Material.

Soil samples were collected and stored from five sites in the west and east side of Traralgon Reservoir catchment as described for Lake Glenbawn. Samples of lignite coal were obtained from Yallourn open-cut mine, next to Yallourn Power Plant and stored in zip-lock bags at 4º C until processed.

Prior to all laboratory analyses, all samples from Lake Glenbawn and Traralgon Railway Reserve were freeze-dried for 72 hours using a Christ Alpha 1–2 LDplus lyophilizer (John Morris Scientific, Sydney, Australia). Grain size and organic matter analyses are presented in Supplementary Material.

Spheroidal carbonaceous particles (SCPs)

Sediment samples were analysed for SCPs using sequential treatments of nitric, hydrofluoric and hydrochloric acids to remove organic, siliceous and carbonate fractions respectively (Rose, 1994). A known fraction of the final suspension in water was then evaporated onto a coverslip, mounted onto a glass slide, and the number of SCPs counted using a light microscope at 400 times magnification. Standard criteria for SCP identification followed Rose (2008) and concentrations were calculated as the number of particles per gram dry mass of sediment (gDM^{-1}). SCP fluxes were calculated as the product of SCP concentration and bulk dry sediment mass accumulation rate (number of particles cm^{-2} yr^{-1}). Analytical blanks and SCP reference material (Rose, 2008) were included with all sample digestions. The detection limit for the technique is typically less than 100 gDM^{-1} and calculated concentrations generally have an accuracy of c. ± 45 gDM^{-1}.

Total mercury analyses

Mercury analyses were conducted using a Milestone Direct Mercury Analyzer (DMA-80 Tri-Cell; Milestone, Bergamo, Italy), following the USEPA method 7473(USEPA, 1998a). Approximately 100 mg of dry sediment, soil or coal was weighed into nickel boats. Two blanks and two Standard Reference Materials (SRMs) were analysed for every 36 samples and a replicate was analysed for every fifth sample. When replicate recovery exceeded a variance of

10% compared to the original sample, a second replicate was run. Certified sediment reference materials NIST-2711a (Montana River Sediment) and SECCC WQB-1 (Lake Ontario) were analysed, and results were in agreement with certified values (7.42 ± 0.18 and 1.06 ± 0.5 mg/kg respectively – more details in Supplementary Table 1).

Total Hg concentrations in trapping sample solutions used for Hg isotope ratio analysis (see below) were also measured at the Tianjin University, China, using a Tekran 2600 cold vapour atomic fluorescence spectrometer (CV-AFS) according to USEPA method 1631E (USEPA, 2002).

Mercury deposition flux:

Mercury flux (μg m^{-2} yr^{-1}) was calculated as Eq. 1:

$$Hgflux = (SR \times 10^{-6}) \times (DBD \times 10^{-2}) \times (Hg \times 10^{-3}) \quad (1)$$

Where SR = sedimentation rate (cm yr^{-1}); DBD = dry bulk density (g cm^{-3}); Hg = Hg concentration (ng g^{-1}). We define Hg flux, in this study, as the ratio of deposition (Hg concentration in ng g^{-1}) to the accumulation rate (sedimentation rate in cm yr^{-1}).

Mercury isotope analyses

Before Hg isotope ratio analysis, all samples were pre-concentrated for Hg by the combustion-trapping method (details in Supplementary Material). The recoveries of samples and CRMs were typically in the range of 85-110%. The trapping solutions were diluted at least two times, and measured for Hg isotope ratios by coupling a customized cold vapour generation system to the multi-collector inductively coupled plasma mass spectrometry (MC-ICPMS, Nu Plasma 3D at Tianjin University, China). The instrumental mass bias was corrected by both an internal NIST 997 Tl standard solution and a bracketed NIST 3133 Hg standard. The bracketed NIST 3133 solutions were matched to the sample solutions to within 10% in both the acid matrix and Hg concentrations. Detailed measurement protocols have been published elsewhere (Sun et al., 2020).

The measured Hg isotope ratio is expressed as δ^{xxx}Hg (‰, xxx = 199, 200, 201, 202, 204):

$$\delta^{xxx}\mathrm{Hg}(‰) = \left[\left({}^{xxx}\mathrm{Hg}/{}^{198}\mathrm{Hg} \right)_{\mathrm{sample}} \Big/ \left({}^{xxx}\mathrm{Hg}/{}^{198}\mathrm{Hg} \right)_{\mathrm{NIST\ 3133}} - 1 \right] \times 1000 \qquad \textbf{(1)}$$

MIF is expressed as Δ^{xxx}Hg notation:

$$\Delta^{xxx}\mathrm{Hg}(‰) = \delta^{xxx}\mathrm{Hg} - {}^{xxx}\beta \times \delta^{202}\mathrm{Hg} \qquad \textbf{(2)}$$

The mass dependent scaling factor ${}^{xxx}\beta$ is 0.2520 for ^{199}Hg, 0.5024 for ^{200}Hg, 0.7520 for ^{201}Hg and 1.4930 for ^{204}Hg.

Mercury isotope ratios of the long-term secondary standard NIST 3177 solution analysed during different analytical sessions between 2018-2019 were -0.52 ± 0.07‰ (2 standard deviation: SD) for δ^{202}Hg, 0.00 ± 0.04‰ (2SD) for Δ^{199}Hg, 0.01 ± 0.03‰ (2SD) for Δ^{200}Hg, and -0.02 ± 0.04‰ (2SD) for Δ^{201}Hg. The NIST 3177 and procedural CRMs (NIST1632e-coal; GSS-5 soil (GBW07405) had Hg isotope ratios in agreement with those reported in previous studies (Sun et al., 2020; Zheng et al., 2020) (Supplementary Table 2). The typical 2σ analytical uncertainties of coal and sediment/soil were estimated as the larger 2SD uncertainties of Hg isotope ratios between NIST 3177 and NIST1632e (i.e., 0.13‰ for δ^{202}Hg, 0.04‰ for Δ^{199}Hg, 0.04‰ for Δ^{200}Hg, and 0.05‰ for Δ^{201}Hg) and between NIST 3177 and GSS-5 i.e., 0.07‰ for δ^{202}Hg, 0.04‰ for Δ^{199}Hg, 0.06‰ for Δ^{200}Hg, and 0.05‰ for Δ^{201}Hg), respectively. The 2SE uncertainties of Hg isotope ratios associated with the sample replicate analyses were applied as the 2σ analytical uncertainties only when they were larger than the typical 2σ analytical uncertainties.

Sediment chronologies

Samples for lead-210 (^{210}Pb) dating were processed at the Australian Nuclear Science and Technology Organisation (ANSTO) by alpha particle spectrometry, following methods described by Harrison et al. (2003). The age-depth models used in this study were obtained by the *Plum* model (Aquino-López et al., 2018) and have already been published elsewhere (Schneider et al., 2020). Influxes of Hg and SCPs (mass sedimentation rate × THg or SCPs) were calculated to account for the differences in sedimentation rate in each of the sediment cores. Details on the dating and age-depth methods are presented in Supplementary Material.

Atmospheric model

Atmospheric transport and deposition of Hg from the two power plants was calculated using version 7 (June 2015) of the CALPUFF modelling system, by the Federal Land Managers' Air Quality Related Values Workgroup (FLAG) (Exponent, 2020; USEPA, 1998b). The CALPUFF input model performs a detailed simulation of the rise of the plume from the power plant's stack, through which the emissions are discharged. The United States Environmental Protection Agency (USEPA) standard default model settings were used throughout. Deposition parameters for Hg, for which there is no default in CALPUFF, were based on USEPA (USEPA, 1997). Details on the model parameters are given in Supplementary Material.

Mercury emissions fed into the CALPUFF model were estimated by multiplying the concentration in coal from the Hunter and Latrobe Valleys (analysed in this study) by the annual consumption of coal per power station. The coal consumption was obtained from the power stations websites for the year 2017 (AGL Energy, 2017a, 2017b; Alinta Energy, 2017; Energy Australia, 2017) and are presented in Supplementary Table 6.

The CALPUFF simulation covered the calendar year 2017. The simulation timestep was one hour. Divalent, elemental and particle-bound Hg were modelled as separate, inert species with different dry and wet deposition characteristics. CALPUFF does not model the chemical transformations of Hg species. However, this is not likely to affect our predicted deposition of Hg in Lake Glenbawn and Traralgon Railway Reservoir due to the short travel time between the emission sources and these reservoirs.

Data analyses

All data analyses were performed using the R Statistical Software (R Development Core Team, 2008). The calculation of catchment area was conducted using the R package OpenSTARS (Kattwinkel and Szocs, 2018), which derives stream networks based on a Digital Elevation Model (DEM) . The sediment age-depth models were obtained using the rplum package (Blaauw et al., 2020). Stratiplots with metal profiles plotted against age were produced using the R package analogue (Simpson, 2007).

■ RESULTS AND DISCUSSION

Age depth models and sedimentation rates

The age-depth models for Lake Glenbawn and Traralgon Railway Reservoir are provided in Supplementary Material (Supplementary Figures S1 and S2). The Lake Glenbawn reservoir was created in 1957 when the Hunter River was dammed and so an age-depth model was constructed down to this date (28 cm) (Supplementary Figure S1). Following impoundment, the mean sedimentation rate was 0.1 g cm^2 yr^{-1}, with no major sedimentary changes occurring. The low sedimentation rate is a result of extensive operations by the NSW Soil Conservation Service that resulted in a stable catchment with minimal soil erosion (Erskine and Bell, 1982). As a result, erosion and catchment inputs are unlikely to have overridden the historical signatures of atmospheric Hg deposition in this lake.

Unsupported ^{210}Pb activities in the Traralgon Reservoir sediment core decreased with depth between 0 and 20 cm and, between 20 and 40 cm depth, the total ^{210}Pb activities were constant (Supplementary Figure S2). Supported ^{210}Pb was estimated from the concentrations of ^{226}Ra (Supplementary Figure S2). The sedimentation rate in this core was around 0.2 g cm^{-2} yr^{-1} above 31 cm and 0.1 g cm^{-2} yr^{-1} below 31cm (Supplementary Table 3). The low sedimentation rates indicate that major erosion events in the catchment are unlikely to have occurred, as this dam has a small catchment size (1.5 km^2) and water in the reservoir originates from a gully ~500 m away.

The concentrations of cobalt, copper, zinc, arsenic, selenium, lead, magnesium and aluminium from both sediment cores were published previously (Schneider et al., 2020). The sediment profiles of these elements indicated that no major erosion has occurred in either catchment. This is further supported by the reasonably constant grain-size of the sediment (illustrated as specific surface area in m^2 g^{-1}) and constant percentage of organic matter within core (Figure 2A-B).

Mercury historical deposition

Lake Glenbawn

Mercury concentrations in the three bituminous coal samples from Newstan mine were measured as 43.0, 46.5 and 40.3 ng g^{-1}. For Lake Glenbawn, Hg concentrations and

deposition fluxes increased from 20 to 74 ng g^{-1} and from 25 to 84 µg m^{-2} yr^{-1}, respectively (Supplementary Table 3). This increase began ~ 1971, at the time when Liddell Power Plant was commissioned. Both Hg concentrations and fluxes reached a peak at around 1989, just before Liddell was retrofitted with bag filters, in 1990 (Figure 2A). From 1990, although coal consumption was still increasing, Hg concentrations and fluxes approximately halved (Hg concentrations decreased from 74 to 37 ng g^{-1}; Hg fluxes decreased from 84 to 40 µg m^{-2} yr^{-1}, Figure 2A), suggesting that the introduction of bag filters was an effective measure taken to control Hg emissions.

Although Bayswater, commissioned in 1986, has a higher electricity production capacity (2,640 MW) than Liddell (2,000 MW). There was minimal increase in Hg deposition to Lake Glenbawn from 1986 and 1990 (Figure 2A). This is likely a result of Bayswater being commissioned with bag filters in place, a more efficient technology to control metal emissions (Yi et al., 2008) than the original electrostatic precipitation technology at Liddell. From 2010 onwards, Hg deposition in Lake Glenbawn remained stable, likely a reflection of the decrease in demand for coal power generation, demonstrated by the data on coal consumption in New South Wales (Figure 2A).

The increase in Hg as a result of the commissioning of the Liddell Power Plant is paralleled by the start of the spheroidal carbonaceous particle (SCP) record in the sediment in the 1970s, (Figure 2A). Although SCP concentrations and fluxes are low, overall, they increase in the sediments of Lake Glenbawn. A decline in SCP concentrations in 1990 corresponds to the time when Liddell was retrofitted with bag filters (Figure 2A). Thereafter, as for Hg, SCP concentration and flux fluctuate with changes in demand for electricity generation although the low concentrations and fluxes exaggerate these patterns (Figure 2A). This is in agreement with previous publications demonstrating correlations between SCP fluxes and other metals emitted by coal-fired power plants (Bindler et al., 2001; Rose et al., 2012; Schneider et al., 2020).

Traralgon Railway Reservoir

The mercury concentration in lignite coal from Yallourn open-cut mine was measured as 70 ng g^{-1}. Mercury concentrations and deposition fluxes in the sediments of Traralgon Railway Reservoir began to increase in the 1970s, when Hazelwood Power Plant was commissioned (Figure 2B, Supplementary Table 3). Concentrations and fluxes further increased gradually as

Yallourn, Loy Yang A and Loy Yang B were commissioned in the Latrobe Valley (Table 1, Figure 2B). In contrast to Lake Glenbawn, Hg deposition in Traralgon increases throughout the core, likely due to a failure to upgrade these power plants with better pollution controls. The only pollution control technology installed in the Latrobe Valley power plants are electrostatic precipitators.

The first appearance of SCP in Traralgon sediments is concurrent with the commissioning of the Hazelwood Power Plant. SCP concentrations increase as other power plants were commissioned (Figure 2B). The most abrupt increase in both Hg and SCP deposition occurred at ~ 2006 and 2014. This increase is unlikely to be a result of an increase in electricity demand, given coal consumption is relatively stable during this period (Figure 2B). Possible causes are fires in the open-cut coal mines in the area in 2006 and 2014. The fire of 2006, at the Hazelwood open cut mine, was exacerbated by strong winds that caused the fire to spread over 2 km of the open cut mine (Catford et al., 2014). The 2014 incident was even more catastrophic, with fire reaching 1,100 hectares of the Hazelwood mine, with a perimeter of 18 kilometres (Asher and Whittaker, 2020; Catford et al., 2014). Although the increase in Hg and SCP are concurrent with the time of the fire, more studies, including air sample filters and soils are required to confirm these as potential sources.

Hunter Valley vs. Latrobe Valley

Overall, sediments from Lake Glenbawn and Traralgon Railway Reservoir have similar background (related to the time before power stations were commissioned) Hg deposition fluxes ($\bar{x}$ = 20.5 ± 2.9 µg m^{-2} yr^{-1} for Lake Glenbawn and $\bar{x}$ = 24.0 ± 2.5 µg m^{-2} yr^{-1} for Traralgon Railway Reservoir, Supplementary Table 4). While Hg deposition fluxes have increased in sediments of Lake Glenbawn by a factor of 2.9 above background following the commissioning of the coal-fired power plants, those at Traralgon have increased by 14-times. This is due to a combination of several factors: (1) Traralgon Reservoir is located just a short distance and within the prevailing wind direction of coal-fired power plants in the Latrobe Valley (Figure 1 A-B); (2) lignite coal has higher Hg concentrations than bituminous coal (70 and 40 ng g^{-1} respectively, Supplementary table 4) and (3) coal-fired power plants from Latrobe Valley (VIC) are less regulated and have less efficient devices to control Hg emissions than power plants in the Hunter Valley (NSW) (Supplementary Material).

Mercury isotope variation

Δ^{199}Hg vs δ^{202}Hg and Δ^{199}Hg vs Δ^{201}Hg values for all samples analysed in this study are plotted in Figure 3. While significant MDF (δ^{202}Hg) and MIF of the odd-mass number isotopes (Δ^{199}Hg and Δ^{201}Hg) were observed for these samples (Supplementary Table 4, Figure 3A), the MIF of even-mass number isotopes (Δ^{200}Hg and Δ^{204}Hg) are insignificant within analytical uncertainty (Supplementary Table 4), and will not be discussed further. The Δ^{199}Hg vs δ^{202}Hg plot (Figure 3A) reveals a clear separation between lignite and bituminous coal, illustrating the distinct isotope ratios of these two coal sources used for power generation.

Hunter Valley

The bituminous coals combusted in Hunter Valley power plants have a mean δ^{202}Hg and Δ^{199}Hg value of -1.98 ± 0.06 ‰ and 0.04 ± 0.01‰ (2SD, n=3), respectively (Figure 4A). They are isotopically distinct from Lake Glenbawn catchment soils, which have more positive δ^{202}Hg (-0.90 ± 0.37 ‰) and more negative Δ^{199}Hg (-0.37 ± 0.10 ‰) (2SD, n=2).

Subsamples from the sediment core have intermediate δ^{202}Hg (-1.12 ± 0.66‰ 2SD) and Δ^{199}Hg (-0.28 ± 0.19 ‰) values. The sediment at 30-31 cm and 32-33 cm depths, before power plant commissioning, had a very similar Hg isotope composition (δ^{202}Hg = -0.91 ± 0.07 ‰; Δ^{199}Hg= -0.43 ± 0.04 ‰, 2SD) to the catchment soils (δ^{202}Hg = -0.90 ± 0.37; Δ^{199}Hg= -0.37 ± 0.10‰, 2 SD), but shifted to more negative δ^{202}Hg and more positive Δ^{199}Hg towards the top of the core (Figure 4A).

The difference in δ^{202}Hg values between Lake Glenbawn catchment soils (-0.91 ± 0.42‰ 2SD) and bituminous coal (-1.98 ± 0.13‰, 2SD) is large (Figure 4A). The more negative δ^{202}Hg value in sediment samples deposited in Lake Glenbawn after the onset of coal-fired power plants, compared to background sediment, suggests an increase in Hg deposition from combusted coal (Figure 4A). A slight positive δ^{202}Hg shift in the stack gas is occurring at 12 cm. This could be a result of the installation of bag filters at Liddell and Bayswater in 1986 and 1990. The increase in δ^{202}Hg value at the top of the sediment core is likely a result of the decrease in electricity production and coal burning over the last decade (DEE, 2018) (Figure 4A).

The difference in Δ^{199}Hg values pre- and post-power plant commissioning (-0.41 ± 0.08 ‰ vs -0.23 ± 0.08 ‰, 2SD) (Figure 4A) also suggests a change in Hg sources, with coal-fired power plant emissions and deposition resulting in more positive Δ^{199}Hg values in sediments deposited after the commissioning of coal-fired power plants.

Latrobe Valley

The lignite sample from the Yallourn open-cut mine has a δ^{202}Hg and Δ^{199}Hg value of -1.95‰ and -0.39‰ (2SD), respectively. When compared to catchment soils (δ^{202}Hg = -1.73 ± 0.42‰; Δ^{199}Hg= -0.52 ± 0.05‰, 2SD, n=5), the lignite is similar in δ^{202}Hg but differs considerably in Δ^{199}Hg. Although sediment samples generally have more positive δ^{202}Hg values than both catchment soils and coal, their Δ^{199}Hg values are within the range of catchment soils and lignite coal (Figure 4B, Supplementary Table 4). The sediment deposited prior to power plant construction (pre-1971) has a more positive δ^{202}Hg value (-1.15 ‰) than post-power plant sediments (-1.52 ± 0.14‰ 2SD) and more negative Δ^{199}Hg (-0.54 ‰) than post-power plant sediments (-0.44 ± 0.5‰ 2SD ‰, n=5). In addition, Δ^{199}Hg differs considerably from catchment soils and the sediment prior to power plants. The Δ^{199}Hg signal in the catchment soils is similar to that of the reservoir sediments deposited prior to power plant construction. This indicates that changes in Δ^{199}Hg in the sediment core are likely a result of Hg deposition from the coal-fired power stations.

For both lakes, older sediments prior to the commissioning of power plants have more negative Δ^{199}Hg values likely because catchment soils had a greater contribution to these older sediments (Figure 4B). Previous studies have also shown that older sediments in lake cores are usually characterised by more negative Δ^{199}Hg values (Biswas et al., 2008; Feng et al., 2010; Yin et al., 2016).

The isotopic data for coals in this study are consistent with isotopic data for coals worldwide in which bituminous coals have higher Δ^{199}Hg values than lignite (Sun et al., 2016a). The Australian bituminous coal analysed in this study (δ^{202}Hg = -1.98 ± 0.06 ‰; Δ^{199}Hg 0.04 ± 0.01‰, 2SD) had Hg isotope compositions comparable to Indian bituminous coals (δ^{202}Hg = -1.87‰; Δ^{199}Hg=0.04‰) reported by Sun et al. (Sun et al., 2016a). The bituminous coals in India and Australia were both formed in the Late Permian, and at that time India and Australia were connected on the Gondwana supercontinent (Powell et al., 1993), where they

may have had similar coal-depositional environments. In contrast, the studied lignite was formed later, in the Cenozoic (Holdgate et al., 2000), when Australia had moved to near its current position (Sutherland, 1995).

Mercury isotope fractionation and source contribution estimation

Mercury isotopic compositions in both Glenbawn Dam and Traralgon Railway Reservoir are within those defined by two primary Hg sources (catchment soils and coal), except δ^{202}Hg values in the sediment core samples from the Traralgon Railway Reservoir (Figure 4B). This suggests that MDF likely occurred during coal combustion (Sun et al., 2014, 2013) and/or Hg deposition into sediments. Furthermore, aqueous Hg sorption onto organic matter and minerals, and biotic and abiotic Hg reduction during and after Hg deposition into sediments can also cause large MDF (Blum et al., 2014; Sun et al., 2019).

In contrast to MDF, large, odd MIF (Δ^{199}Hg) mainly occurs during photochemical processes. Coal combustion and non-photochemical processes do not induce MIF (Sun et al., 2014). The odd MIF signatures of sediments in this study define a linear regression slope of ~1 (Figure 3B), with coal and catchment soils plotted against the regression line. This suggests that the odd-MIF in all our samples are derived from Hg that had undergone photochemical reduction. Overall, compared to δ^{202}Hg, Δ^{199}Hg is a more robust indicator to discriminate Hg sources in the Hunter and Latrobe Valley.

Based on these arguments, we used Δ^{199}Hg as a conservative tracer to build a binary mixing model (Sun et al., 2020) to quantify Hg contributions from different sources. For both lakes, the fraction contribution of Hg from soil catchment to lake sediments was higher and more certain at the bottom of the core (93% for Glenbawn and 87% for Traralgon, Supplementary Table 5). For sediment deposited after the commissioning of coal-fired power plants, the binary mixing model estimated that 34% and 66% of Hg in Lake Glenbawn and 61% and 39% of Hg in Traralgon Reservoir was derived from the soil catchment and coal-fired power plants, respectively. This calculation suggests that whilst soil is most likely the main source of Hg for the bottom of the core (pre-power plant), coal contributes significantly to the anthropogenic Hg deposited after the power plants were commissioned.

Mercury atmospheric model

By simulating the power plants using CALPUFF, 3-dimensional air concentration fields of each Hg species were obtained (Supplementary Table 6). Atmospheric mercury (Hg) is categorised into elemental Hg (Hg^0), reactive gaseous or oxidized Hg (RGM) and particulate Hg (HgP) (Elgazali et al., 2018). For the Hunter Valley, approximately 176 kg of Hg^0, 191 kg of RGM and 1.4 kg of HgP is estimated to be emitted per year (Supplementary Table 6). For the Latrobe Valley, 1752 kg of Hg^0, 1898 kg of RGM and 13 kg of HgP is estimated to be emitted per year (Supplementary Table 6).

The estimates of total Hg emissions indicates that power stations in the Latrobe Valley emit 10 X more Hg (3664 kg yr^{-1}) than power stations in the Hunter Valley (369 kg yr^{-1}) (Supplementary Table 6). This result can be explained by the type of coal burnt in the Latrobe Valley, as lignite coal has a higher Hg content than bituminous coal used by power stations in the Hunter Valley (Supplementary Table 6). Furthermore, the power plants in the Latrobe Valley use less efficient pollution control device (electrostatic precipitator) than power stations in the Hunter Valley.

The spatial annual total mercury deposition (µg m^{-2} yr^{-1}) in the two areas (5A-B), and the total mercury deposition (µg m^{-2} yr^{-1}) by distance (km) from power plants (5C-D) are shown in Figure 5 and Supplementary Table 6. The results of Hg deposition obtained from the atmospheric model are similar to the Hg deposition fluxes recorded in sediments of Lake Glenbawn (~50 µg m^{-2} yr^{-1}) and Traralgon Railway Reservoir (~200 µg m^{-2} yr^{-1}) (Figure 2A-B, Figure 5A-D, Supplementary Tables 3 and 6). For both Valleys, 50% of the Hg emitted is deposited within 50 km from the source (Supplementary Table 6).

Previous study in the Latrobe Valley (Emmerson et al., 2015) simulated Hg deposition from the same power plants included in our work. The monthly maximum local deposition rate according to Emmerson et al. (2015) is 0.5 ug m^{-2} mth^{-1} in March 2005, 5-10 km from the power plants. They used a model with 3-km horizontal resolution. To make our result comparable, we calculated maximum deposition rates averaged over 3km x 3 km areas from our results, yielding a predicted maximum deposition rate in March, using 2017 meteorological data, of 27 ug m^{-2} mth^{-1} .

Our annual modelled Hg emission rate was 52 times higher than Emmerson et al (2015) result. The main difference between our work and that of Emmerson et al (2015) is the input data into the model. We used measured Hg content in coal, and reported coal consumption data by the power plants while Emmerson et al (2015) used the Nelson et al. (2012)

atmospheric Hg emission inventory. Our model total mercury emissions rates estimate of 3660 kg yr^{-1} is 35 times higher than 101 kg yr^{-1} used by Emmerson et al (2015).

The emission rates of RGM in our study are 47 times higher than Emmerson (2015). We modelled 1900 kg yr^{-1} while Emmerson et al. (2015) modelled 40 kg yr^{-1}. The difference in THg and RGM emission rates between our model and Emmerson (2015) is consistent (52 times higher for THg and 47 times higher for RGM).

Schofield et al (2021) measured ground-level air concentrations of Hg at a location 5 km to the south of Hazelwood power station, and 14 and 18 km from the two other power stations, finding averages of 1.2–1.3 ng m^{-3} during daytime and 1.6–1.8 ng m^{-3} during night time in June 2013. Concentrations predicted by our modelling at their sampling location in June are 0.06 ng m^{-3}. This represents a small fraction of the ground-level air concentrations (which is the sum of the soil re-emissions and the emissions from the stack). This supports the authors' conclusion that most airborne mercury at the ground level is associated with re-emission from soils, rather than direct emissions from power plant stacks.

Regulatory implications

The sediment analyses and atmospheric model in this study show much higher Hg emission and deposition in the Latrobe Valley than in the Hunter Valley. This pattern is consistent with the different regulatory approaches adopted in Victoria and NSW, with coal-fired power plants in the former not required to limit Hg emissions and also not required (until very recently) to specifically limit Hg emissions. Victoria also does not require the adoption of bag filters to reduce Hg emissions (details of regulatory framework for both states are given in Supplementary Material). In particular, the results of this study reveal that retrofitting the Liddell power plant in the Hunter Valley with bag filters coincided with a two-fold decrease in Hg deposition in Lake Glenbawn (Figure 2A). This result suggests there is a significant impact from installing more effective pollution control technology to limit Hg emissions and deposition in the environment. If coal-fired power plants in Australia were to adopt international best practice (e.g., wet flue gas desulfurization) in emissions control technology, it is expected that Hg emissions and deposition would decrease even further.

Furthermore, Australia has signed but not ratified the Minamata Convention on Mercury (Sinclair and Schneider, 2019), an international treaty to reduce Hg use and emissions. If and when Australia ratifies the Convention, it will be legally bound to take steps to reduce Hg

emissions, including those from coal-fired power plants. While the Convention allows for a phased approach to Hg reduction plans, it will focus attention on how, and to what extent, state jurisdictions in Australia address Hg emissions. Historically, coal-fired power plants in Victoria have not been required to limit Hg emissions. On 5 March 2021, Environment Protection Authority Victoria announced the introduction of limits for mercury, fine particles (PM2.5) and coarse particles (PM10) for coal fired power stations in Victoria (EPA VIC, 2021). The power station will also be required to continuously monitor air emissions, and report on these publicly. However, they will not be required to install fabric (bag) filters as has been required in NSW. The results of this study suggest basic pollution control technologies are linked to tangible reductions in Hg emissions from coal power plants, and that even though retrofitting and installing new technologies is costly (Australian Energy Council, 2019), doing so can lead to substantial reductions in Hg emission.

Future directions

The Hg isotope data presented in this study are the first published for the Australian environment and represent an important first step towards tracing sources of Hg emissions. Isotopic analyses of more coal samples are needed in order to develop the use of Hg isotope data and mixing models to determine the coal contributing to Hg deposited in the environment. This method can be applied to identify sources of Hg in the environment across Australia.

While we argue that coal-fired power plant emissions are the dominant source of "new" Hg deposited in these two lakes, this statement comes with the caveat that there are a limited number of coal measurements. More samples are needed to better define the isotopic signature of the Australian coal. Coals from other states should also be considered, particularly in Queensland and South Australia which are also significant producers of electricity from coal combustion (Hardisty et al., 2012). Mercury isotopic signatures from other industrial activities and processes in Australia should also be studied (e.g. metal smelting, cement production and even bushfires) to allow a better discernment of Hg sources in the country.

Author contribution statement

L Schneider and S. Haberle conceived the original idea for this project. L. Schneider, A. Lintern and S. Haberle planned and performed field work in the Latrobe Valley. L. Schneider, D. Sinclair and C. Holley performed field work in the Hunter Valley. L Schneider processed samples for mercury analyses and interpretation of the data. N. Rose and L. Schneider performed analyses of spheroidal carbonaceous particles. L. Myllyvirta performed and discussed the atmospheric model data. N. Rose and A. Lintern verified the analytical methods used in this study. A. Lintern and A. Zawadzki performed ^{210}Pb dating analyses. D Sinclair and C. Holley researched the pertinent regulatory framework on metal emissions in Australia and discussed the regulatory section of this manuscript. All authors discussed the results and contributed to the final manuscript.

Declaration of competing interest

The authors declare that they have no known competing financial interests or personal relationships that could have appeared to influence the work reported in this paper.

Acknowledgements

This project was financially supported by the Australian Research Council (award: DE180100573), The Asia Pacific Innovation Program (APIP) 2018 and 2019 and the Australia Nuclear Science and Technology Organisation (award: AP11653 2018-2). We would like to thank the Traditional Owners both past and present for their support in allowing us to work on their lands. Nicholas Metherall assisted with fieldwork in the Latrobe Valley and Bill Maher and Jaimie Potts assisted with fieldwork in the Hunter Valley. We thank Gary Deane for the information on the Traralgon Railway Reservoir hydrology and Simon Clark (Latrobe City Council) for providing access to the collection of sediment. Martin O'Brien (Water NSW) has kindly provided access for sediment collection at Lake Glenbawn. Robert Lane, Ross Cayley and Christopher Osborne, from Geological Survey Victoria, have provided information on the geological formation of Traralgon Railway Reservoir.

■ REFERENCES

AGL Energy, 2017a. Loy Yang Power Station | AGL [WWW Document]. URL https://www.agl.com.au/about-agl/how-we-source-energy/loy-yang-power-station (accessed 5.14.21).

AGL Energy, 2017b. AGL Macquarie | Liddell & Bayswater Power Stations | AGL [WWW Document]. URL https://www.agl.com.au/about-agl/how-we-source-energy/agl-macquarie (accessed 5.14.21).

Alinta Energy, 2017. Home [WWW Document]. Loy Yang B. URL https://www.loyyangb.com.au/ (accessed 5.14.21).

Aquino-López, M.A., Blaauw, M., Christen, J.A., Sanderson, N.K., 2018. Bayesian Analysis of ^{210}210Pb Dating. JABES 23, 317–333. https://doi.org/10.1007/s13253-018-0328-7

623 Asher, N., Whittaker, J., 2020. Hazelwood mine operators fined $1.9 million over blaze that burned
624 for 45 days [WWW Document]. URL https://www.abc.net.au/news/2020-05-19/hazelwood-
625 power-station-latrobe-valley-2014-mine-fire-fine/12261858 (accessed 6.15.20).
626 Australia Government Regional Assessment Program, 2019. Brown coal -Bioregional Assessments -
627 Latrobe Valley [WWW Document]. URL
628 https://www.bioregionalassessments.gov.au/assessments/12-resource-assessment-
629 gippsland-basin-bioregion/12112-brown-coal (accessed 5.17.19).
630 Australian Energy Council, 2019. Considerations for retrofitting emissions control systems in
631 Australian coal power plants. Australian Energy Council, Brisbane, QLD.
632 Bergquist, B., Blum, J.D., 2007. Mass-Dependent and -Independent Fractionation of Hg Isotopes by
633 Photoreduction in Aquatic Systems. Science 318, 417–420.
634 Biester, H., Bindler, R., Martinez-Cortizas, A., Engstrom, D.R., 2007. Modeling the Past Atmospheric
635 Deposition of Mercury Using Natural Archives. Environ. Sci. Technol. 41, 4851–4860.
636 https://doi.org/10.1021/es0704232
637 Bindler, R., Renberg, I., Appleby, P.G., Anderson, N.J., Rose, N.L., 2001. Mercury Accumulation Rates
638 and Spatial Patterns in Lake Sediments from West Greenland: A Coast to Ice Margin
639 Transect. Environ. Sci. Technol. 35, 1736–1741. https://doi.org/10.1021/es0002868
640 Biswas, A., Blum, J.D., Bergquist, B.A., Keeler, G.J., Xie, Z., 2008. Natural Mercury Isotope Variation in
641 Coal Deposits and Organic Soils. Environ. Sci. Technol. 42, 8303–8309.
642 https://doi.org/10.1021/es801444b
643 Blaauw, M., Christen, J.A., Aquino-López, M.A., Esquivel-Vazquez, J., Gonzales, O.M., Belding, T.,
644 Theiler, J., Gough, B., Karney, C., 2020. Bayesian Age-Depth Modelling of '210Pb'-Dated
645 Cores (No. version 0.1.4), R package.
646 Blum, J.D., Sherman, L.S., Johnson, M.W., 2014. Mercury Isotopes in Earth and Environmental
647 Sciences. Annual Review of Earth and Planetary Sciences 42, 249–269.
648 https://doi.org/10.1146/annurev-earth-050212-124107
649 BOM, 2019. Wind Roses - Australian Bureau of Meteorology [WWW Document]. URL
650 http://www.bom.gov.au/climate/averages/wind/wind_rose.shtml (accessed 5.13.19).
651 Catford, B., Catford, J., Petering, S., 2014. Hazelwood Mine Fire Inquiry report 2014. Melbourne, VIC,
652 Australia.
653 Dabrowski, J.M., Ashton, P.J., Murray, K., Leaner, J.J., Mason, R.P., 2008. Anthropogenic mercury
654 emissions in South Africa: Coal combustion in power plants. Atmospheric Environment 42,
655 6620–6626. https://doi.org/10.1016/j.atmosenv.2008.04.032
656 DEE, 2018. Australian electricity generation, by fuel type, physical units (No. Table O, April 2018).
657 Department of the Environment and Energy, Australian Energy Statistics, Canberra, A.C.T.
658 Australia.
659 Dutt, U., Nelson, P.F., Morrison, A., Strezov, V., 2009. Mercury wet deposition: an Australian study to
660 assess impact of coal-fired power stations. Fuel Processing Technology 90, 1354–1359.
661 Elgazali, A.A.S., Gajdosechova, Z., Abbas, Z., Lombi, E., Scheckel, K.G., Donner, E., Fiedler, H.,
662 Feldmann, J., Krupp, E.M., 2018. Reactive gaseous mercury is generated from chloralkali
663 factories resulting in extreme concentrations of mercury in hair of workers. Scientific
664 Reports 8, 3675. https://doi.org/10.1038/s41598-018-20544-5
665 Emmerson, K.M., Cope, M.E., Lee, S., Hibberd, M.F., Torre, P., 2015. Modelling atmospheric mercury
666 from power stations in the Latrobe Valley, Victoria. Air Quality and Climate Change 49, 5.
667 Energy Australia, 2017. Yallourn Power Station [WWW Document]. EnergyAustralia. URL
668 https://www.energyaustralia.com.au/about-us/energy-generation/yallourn-power-station
669 (accessed 5.14.21).
670 Engstrom, D.R., Fitzgerald, W.F., Cooke, C.A., Lamborg, C.H., Drevnick, P.E., Swain, E.B., Balogh, S.J.,
671 Balcom, P.H., 2014. Atmospheric Hg Emissions from Preindustrial Gold and Silver Extraction
672 in the Americas: A Reevaluation from Lake-Sediment Archives. Environ. Sci. Technol. 48,
673 6533–6543. https://doi.org/10.1021/es405558e

EPA VIC, 2021. EPA finalises power station licence review | Environment Protection Authority Victoria [WWW Document]. URL https://www.epa.vic.gov.au/about-epa/news-media-and-updates/news-and-updates/epa-finalises-power-station-licence-review (accessed 5.16.21).
Erskine, W., Bell, F.C., 1982. Rainfall, floods and river channel changes in the upper Hunter. Aust Geog Studies 20, 183–196. https://doi.org/10.1111/j.1467-8470.1982.tb00403.x
Exponent, 2020. CALPUFF Regulatory Status [WWW Document]. URL http://www.src.com/calpuff/regstat.htm (accessed 8.18.20).
Feng, X., Foucher, D., Hintelmann, H., Yan, H., He, T., Qiu, G., 2010. Tracing Mercury Contamination Sources in Sediments Using Mercury Isotope Compositions. Environmental Science & Technology 44, 3363–3368. https://doi.org/10.1021/es9039488
Gustin, M.S., Amos, H.M., Huang, J., Miller, M.B., Heidecorn, K., 2015. Measuring and modeling mercury in the atmosphere: a critical review. Atmos. Chem. Phys. 15, 5697–5713. https://doi.org/10.5194/acp-15-5697-2015
Hardisty, P.E., Clark, T.S., Hynes, R.G., 2012. Life Cycle Greenhouse Gas Emissions from Electricity Generation: A Comparative Analysis of Australian Energy Sources. Energies 5, 872–897. https://doi.org/10.3390/en5040872
Harrison, J., Heijnis, H., Caprarelli, G., 2003. Historical pollution variability from abandoned mine sites, Greater Blue Mountains World Heritage Area, New South Wales, Australia. Env Geol 43, 680–687. https://doi.org/10.1007/s00254-002-0687-8
Holdgate, G.R., Wallace, M.W., Gallagher, S.J., Taylor, D., 2000. A review of the Traralgon Formation in the Gippsland Basin — a world class brown coal resource. International Journal of Coal Geology 45, 55–84. https://doi.org/10.1016/S0166-5162(00)00020-3
Howard, D., Nelson, P.F., Edwards, G.C., Morrison, A.L., Fisher, J.A., Ward, J., Harnwell, J., van der Schoot, M., Atkinson, B., Chambers, S.D., Griffiths, A.D., Werczynski, S., Williams, A.G., 2017. Atmospheric mercury in the Southern Hemisphere tropics: seasonal and diurnal variations and influence of inter-hemispheric transport. Atmos. Chem. Phys. 17, 11623–11636. https://doi.org/10.5194/acp-17-11623-2017
Jackson, T.A., Muir, D.C.G., 2012. Mass-dependent and mass-independent variations in the isotope composition of mercury in a sediment core from a lake polluted by emissions from the combustion of coal. Science of The Total Environment 417–418, 189–203. https://doi.org/10.1016/j.scitotenv.2011.12.040
Kattwinkel, M., Szocs, E., 2018. openSTARS: An Open Source Implementation of the “ArcGIS” Toolbox “STARS.”
Nelson, P.F., 2007. Atmospheric emissions of mercury from Australian point sources. Atmospheric Environment 41, 1717–1724. https://doi.org/10.1016/j.atmosenv.2006.10.029
Nelson, P.F., Morrison, A.L., Malfroy, H.J., Cope, M., Lee, S., Hibberd, M.L., Meyer, C.P. (Mick), McGregor, J., 2012. Atmospheric mercury emissions in Australia from anthropogenic, natural and recycled sources. Atmospheric Environment 62, 291–302. https://doi.org/10.1016/j.atmosenv.2012.07.067
NSW Planning and Environment, 2019. NSW coalfields - NSW Resources and Geoscience [WWW Document]. URL https://www.resourcesandgeoscience.nsw.gov.au/landholders-and-community/minerals-and-coal/geoscience-for-landholders/coalfields (accessed 5.17.19).
Pavlish, J.H., Sondreal, E.A., Mann, M.D., Olson, E.S., Galbreath, K.C., Laudal, D.L., Benson, S.A., 2003. Status review of mercury control options for coal-fired power plants. Fuel Processing Technology, Mercury Control in Coal-Fired Power Stations 82, 89–165. https://doi.org/10.1016/S0378-3820(03)00059-6
Pinetown, K.L., Faiz, M.M., Saghafi, A., Stalker, L., Holst, J. van, 2008. Coal Seam Gas Distribution in the Hunter Coalfield, Sydney Basin. Petroleum Exploration Society of Australia (PESA), Sydney, NSW. Australia.
Powell, C.M., Li, Z.X., McElhinny, M.W., Meert, J.G., Park, J.K., 1993. Paleomagnetic constraints on timing of the Neoproterozoic breakup of Rodinia and the Cambrian formation of Gondwana.

Geology 21, 889–892. https://doi.org/10.1130/0091-7613(1993)021<0889:PCOTOT>2.3.CO;2
R Development Core Team, 2008. R Development Core Team (2017). R: A language and environment for statistical computing. R Foundation for Statistical Computing, Vienna, Austria. ISBN 3-900051-07-0, URL http://www.R-project.org.
Rose, N.L., 2008. Quality control in the analysis of lake sediments for spheroidal carbonaceous particles. Limnology and Oceanography: Methods 6, 172–179. https://doi.org/10.4319/lom.2008.6.172
Rose, N.L., 2001. Fly-ash particles, in: Last, W.M., Smol, J.P. (Eds.), Tracking Environmental Change Using Lake Sediments: Volume 2: Physical and Geochemical Methods, Developments in Paleoenvironmental Research, Tracking Environmental Change Using Lake Sediments. Springer Netherlands.
Rose, N.L., 1994. A note on further refinements to a procedure for the extraction of carbonaceous fly-ash particles from sediments. J Paleolimnol 11, 201–204. https://doi.org/10.1007/BF00686866
Rose, N.L., Yang, H., Turner, S.D., Simpson, G.L., 2012. An assessment of the mechanisms for the transfer of lead and mercury from atmospherically contaminated organic soils to lake sediments with particular reference to Scotland, UK. Geochimica et Cosmochimica Acta, Environmental Records of Anthropogenic Impacts 82, 113–135. https://doi.org/10.1016/j.gca.2010.12.026
Schneider, L., Rose, N.L., Lintern, A., Sinclair, D., Zawadzki, A., Holley, C., Aquino-López, M.A., Haberle, S., 2020. Assessing environmental contamination from metal emission and relevant regulations in major areas of coal mining and electricity generation in Australia. Science of The Total Environment 728, 137398. https://doi.org/10.1016/j.scitotenv.2020.137398
Scire, J.S., Strimaitis, D.G., Yamartino, R.J., 2000. Scire, J.S., Strimaitis, D.G., Yamartino, R.J., 2000. A User's Guide for the CALPUFF Dispersion Model (Version 5). Earth Tech Inc. 521.
Selin, N.E., 2009. Global Biogeochemical Cycling of Mercury: A Review. Annual Review of Environment and Resources 34, 43–63. https://doi.org/10.1146/annurev.environ.051308.084314
Simpson, G.L., 2007. Analogue Methods in Palaeoecology: Using the analogue Package. Journal of Statistical Software 22, 1–29.
Sinclair, D., Schneider, L., 2019. Mercury Emissions, Regulation and Governance of Coal-fired Power Stations in Victoria, Australia. Environmental and Planning Law Journal 36, 630–641.
Stock, A., 2014. Australia's Electricity Sector: Ageing, Inefficient and Unprepared. Climate Council of Australian Ltd, Potts Point , NSW.
Sun, R., Heimbürger, L.-E., Sonke, J.E., Liu, G., Amouroux, D., Berail, S., 2013. Mercury stable isotope fractionation in six utility boilers of two large coal-fired power plants. Chemical Geology, Advances in mercury stable isotope biogeochemistry 336, 103–111. https://doi.org/10.1016/j.chemgeo.2012.10.055
Sun, R., Jiskra, M., Amos, H.M., Zhang, Y., Sunderland, E.M., Sonke, J.E., 2019. Modelling the mercury stable isotope distribution of Earth surface reservoirs: Implications for global Hg cycling. Geochimica et Cosmochimica Acta 246, 156–173. https://doi.org/10.1016/j.gca.2018.11.036
Sun, R., Sonke, J.E., Heimbürger, L.-E., Belkin, H.E., Liu, G., Shome, D., Cukrowska, E., Liousse, C., Pokrovsky, O.S., Streets, D.G., 2014. Mercury Stable Isotope Signatures of World Coal Deposits and Historical Coal Combustion Emissions. Environ. Sci. Technol. 48, 7660–7668. https://doi.org/10.1021/es501208a
Sun, R., Sonke, J.E., Liu, G., 2016a. Biogeochemical controls on mercury stable isotope compositions of world coal deposits: A review. Earth-Science Reviews 152, 1–13. https://doi.org/10.1016/j.earscirev.2015.11.005
Sun, R., Streets, D.G., Horowitz, H.M., Amos, H.M., Liu, G., Perrot, V., Toutain, J.-P., Hintelmann, H., Sunderland, E.M., Sonke, J.E., 2016b. Historical (1850–2010) mercury stable isotope

776 inventory from anthropogenic sources to the atmosphere. Elem Sci Anth 4, 000091.
777 https://doi.org/10.12952/journal.elementa.000091
778 Sun, R., Yuan, J., Sonke, J.E., Zhang, Y., Zhang, T., Zheng, W., Chen, S., Meng, M., Chen, J., Liu, Y.,
779 Peng, X., Liu, C., 2020. Methylmercury produced in upper oceans accumulates in deep
780 Mariana Trench fauna. Nature Communications 11, 3389. https://doi.org/10.1038/s41467-
781 020-17045-3
782 Sutherland, R., 1995. The Australia-Pacific boundary and Cenozoic plate motions in the SW Pacific:
783 Some constraints from Geosat data. Tectonics 14, 819–831.
784 https://doi.org/10.1029/95TC00930
785 UNEP, 2019. Global Mercury Assessment 2018. Environment Programme, Chemicals and Health
786 Branch, Geneva, Switzerland.
787 USEPA, 2002. Method 1631, Revision E: Mercury in Water by Oxidation, Purge and Trap, and Cold
788 Vapor Atomic Fluorescence Spectrometry (No. EPA-821-R-02-019). United States
789 Environmental Protection Agency, Washington, DC. USA.
790 USEPA, 1998a. Method 7473 - Mercury in solids and solutions by thermal decomposition,
791 amalgamation, and atomic absorption spectrophotometry (No. SW-846-). US Environmental
792 Protection Agency, Washington, D.C.
793 USEPA, 1998b. Interagency Workgroup on Air Quality Modeling (IWAQM) Phase 2 Summary Report
794 and Recommendations for Modeling Long Range Transport Impacts. EPA, Research Triangle
795 Park, North Carolina - USA.
796 USEPA, 1997. Mercury Study-Report to Congress, Volume III: Fate and Transport of Mercury in the
797 Environment. (No. EPA-452/R-97-005). United States Environmental Protection Agency,
798 Washington, DC. USA.
799 Wang, Y., Duan, Y., Yang, L., Jiang, Y., Wu, C., Wang, Q., Yang, X., 2008. Comparison of mercury
800 removal characteristic between fabric filter and electrostatic precipitators of coal-fired
801 power plants. Journal of Fuel Chemistry and Technology 36, 23–29.
802 https://doi.org/10.1016/S1872-5813(08)60009-2
803 Weller, S., Sheehan, P., Tomaney, J., 2011. The regional effects of pricing arbon emissions: an
804 adjustment atrategy for the Latrobe Valley. Centre for Strategic Economic Studies, Victoria
805 University.
806 Yi, H., Hao, J., Duan, L., Tang, X., Ning, P., Li, X., 2008. Fine particle and trace element emissions from
807 an anthracite coal-fired power plant equipped with a bag-house in China. Fuel 87, 2050–
808 2057. https://doi.org/10.1016/j.fuel.2007.10.009
809 Yin, R., Lepak, R.F., Krabbenhoft, D.P., Hurley, J.P., 2016. Sedimentary records of mercury stable
810 isotopes in Lake Michigan. Elem Sci Anth 4, 000086.
811 https://doi.org/10.12952/journal.elementa.000086
812 Zheng, X., Dai, S., Nechaev, V., Sun, R., 2020. Environmental perturbations during the latest Permian:
813 Evidence from organic carbon and mercury isotopes of a coal-bearing section in Yunnan
814 Province, southwestern China. Chemical Geology 549, 119680.
815 https://doi.org/10.1016/j.chemgeo.2020.119680
816

817

818 **Figure and Table Captions:**

819 Table 1 – Power Plant, location, commissioning date, electrical capacity (MW), coal type used
820 and pollution control devices in coal-fired power plants of the Latrobe and Hunter Valleys.

Power Plant	Location	Commissioned	Electrical capacity (MW)	Feed coal	Pollution Control Device

Bayswater	Hunter Valley	1985	2,640	bituminous	Bag filter
Liddell	Hunter Valley	1971	2,000	bituminous	Bag filter
Loy Yang A	Latrobe Valley	1984	2,210	lignite	Electrostatic precipitator
Loy Yang B	Latrobe Valley	1993	1,070	lignite	Electrostatic precipitator
Yallourn	Latrobe Valley	1975	1,480	lignite	Electrostatic precipitator
Hazelwood	Latrobe Valley	1961 - 2017	1200	lignite	Electrostatic precipitator

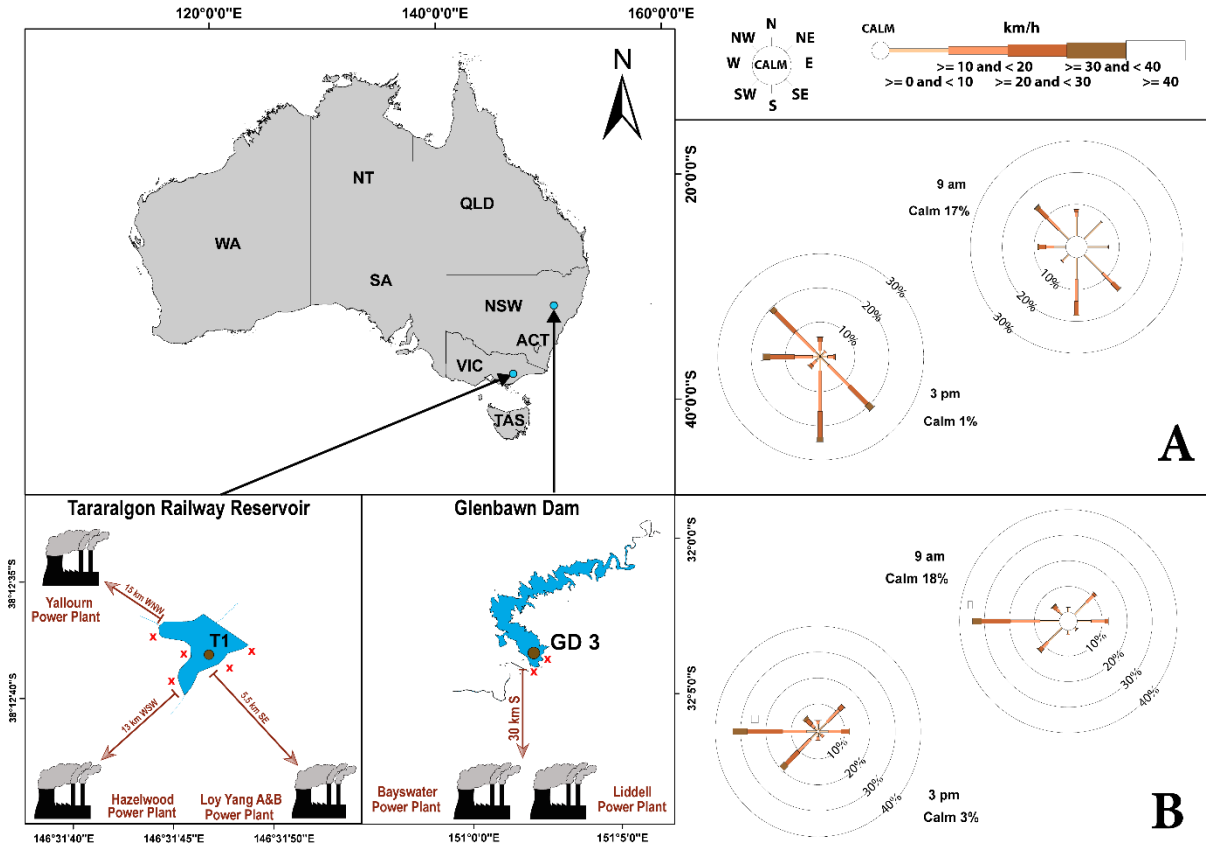

Figure 1 - Map of Australia showing the locations of Traralgon Railway Reservoir (Latrobe Valley) in Victoria and Lake Glenbawn (Hunter Valley) in New South Wales. Sediment sampling sites in Traralgon Railway Reservoir and Lake Glenbawn are indicated by brown circles within lakes. The distance from power plants in relation to the lakes are indicated by brown arrows. Red "Xs" indicate the location of catchment soil samples. Wind roses show the frequency of occurrence of wind speed and direction for 9 am and 3 pm annually at A) Scone Airport (annual average between 1991 and 2010, 14 km west of Lake Glenbawn and B) Latrobe Valley airport (annual average between 1984 and 2019), 5 km west of Traralgon Railway Reservoir. The percentage of calm conditions is represented by the size of the centre circle - the bigger the circle, the higher the frequency of calm conditions. The length of each segment

within a branch is proportional to the frequency of winds blowing within the corresponding range of speeds from that direction. From: Australian Bureau of Meteorology (BOM, 2019).

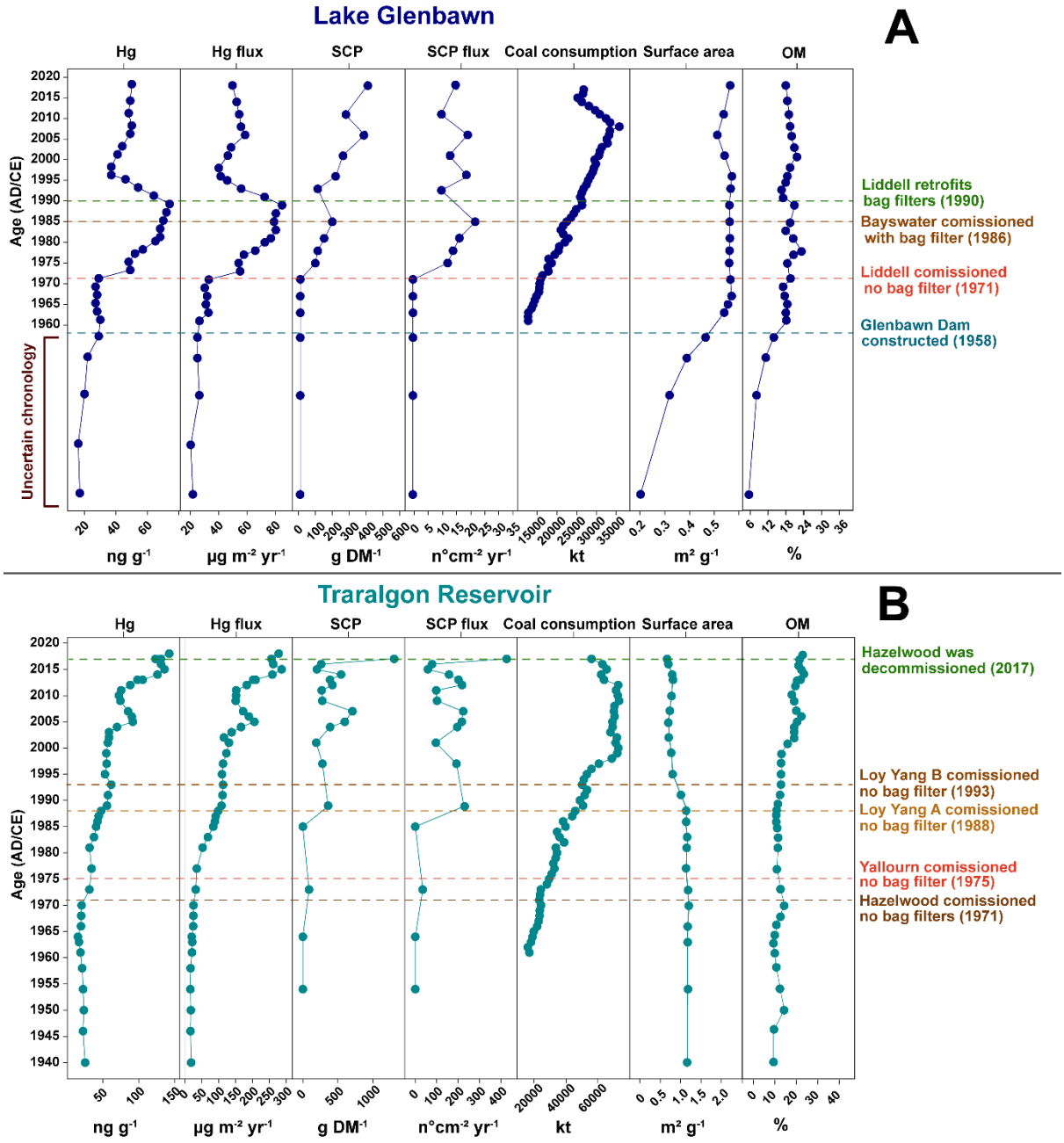

Figure 2 – Lake Glenbawn (A) sediment data: mercury (Hg) concentration (ng g^{-1}), Hg flux (µg m^{-2} yr^{-1}), spheroidal carbonaceous particles (SCP) concentration (g DM^{-1}), SCP flux (nº cm^{-2} yr^{-1}), black coal consumption in New South Wales (kt) (source: Australian Energy Statistics, Table P (DEE, 2018)), Specific Surface Area (m^2 g^{-1}) and organic matter (OM, %), (B) Traralgon Railway Reservoir sediment data: mercury concentration (ng g^{-1}), Hg flux (µg m^{-2} yr^{-1}), spheroidal carbonaceous particles (SCP) concentration (g DM^{-1}), SCP flux (nº cm^{-2} yr^{-1}), brown coal consumption in Australia (kt)) (source: Australian Energy Statistics, Table P (DEE, 2018)), specific surface area (m^2 g^{-1}) and organic matter (OM, %).

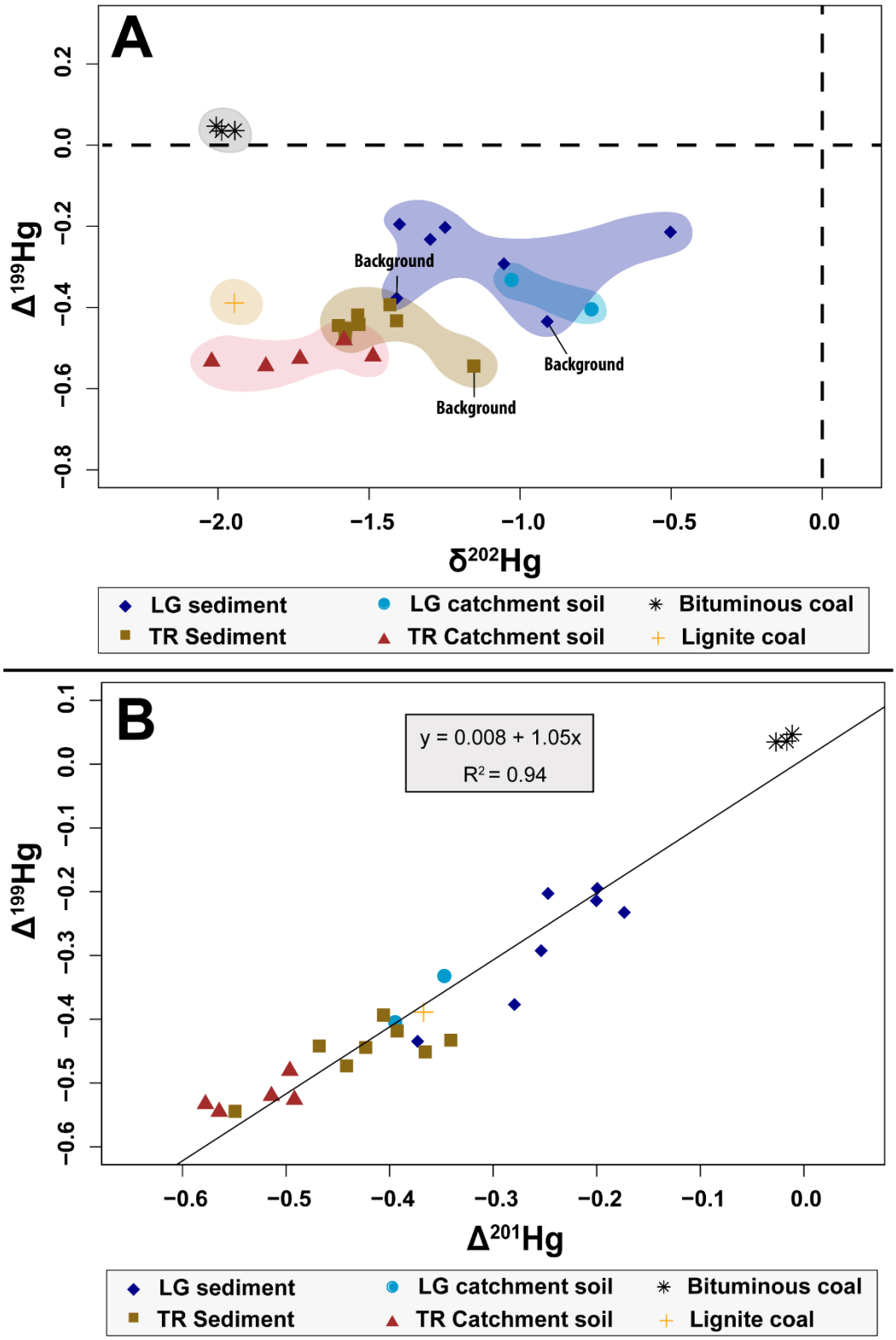

Figure 3 – Mercury isotope plots of catchment soil, lake sediment and coal samples: A) $\Delta^{199}Hg$ vs $\delta^{202}Hg$. Samples are grouped by sample types in the form of shaded areas; B) $\Delta^{199}Hg$ vs $\Delta^{201}Hg$. LG stands for Lake Glenbawn and TR stands for Traralgon Railway Reservoir.

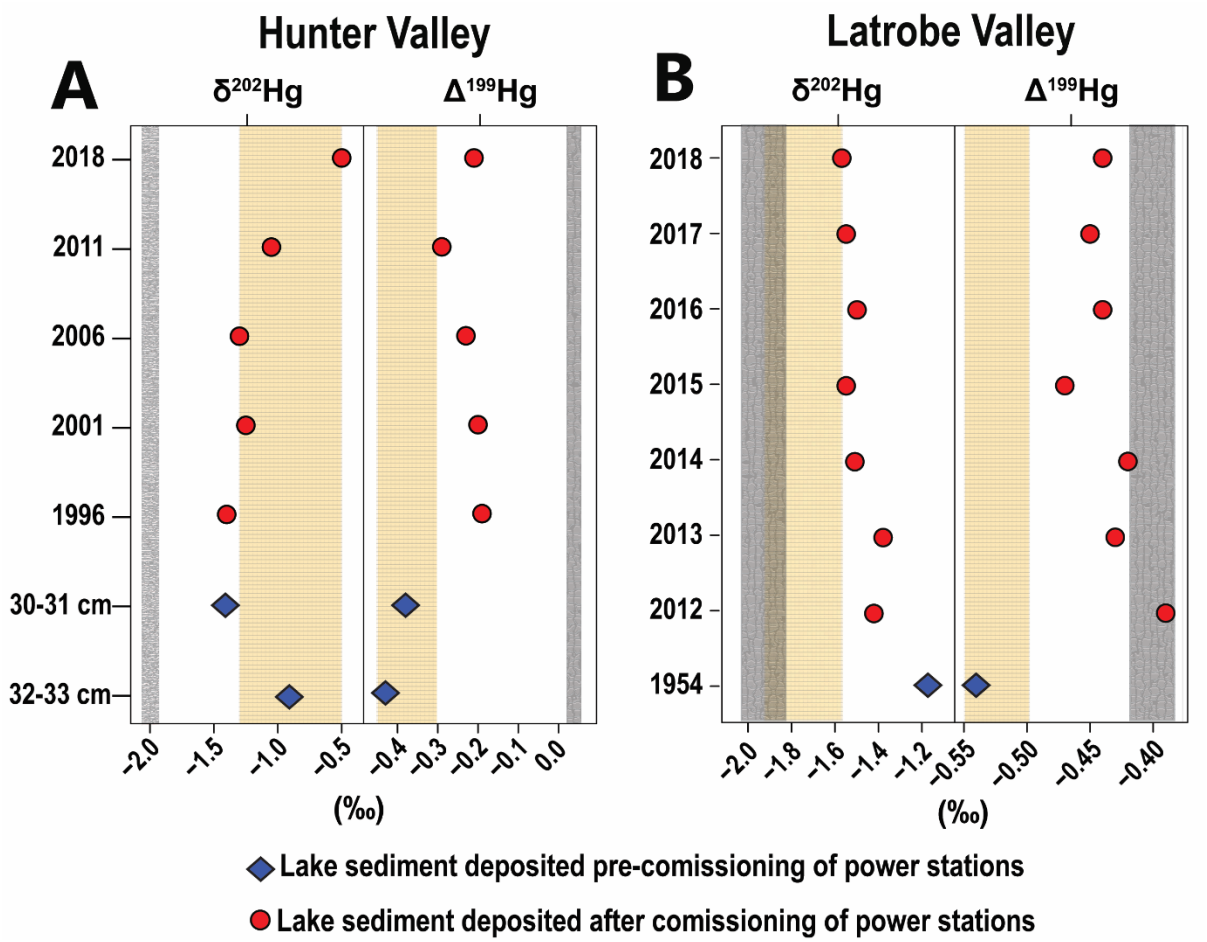

Figure 4 - Isotopic data for $\delta^{202}Hg$ and $\Delta^{199}Hg$ in sediments deposited before and after commissioning of coal-fired power plants in: A) Lake Glenbawn, Hunter Valley, New South Wales and B) Traralgon Railway Reservoir, Latrobe Valley, Victoria. The range of isotopic values from coal are indicated as a grey vertical bar, and from catchment soil as a yellow vertical bar. The isotopic range was calculated as the mean isotopic values ± 2SD. As only one lignite coal sample was analysed, the typically analytic 2σ uncertainty was used to calculate the isotopic range plotted in this figure.

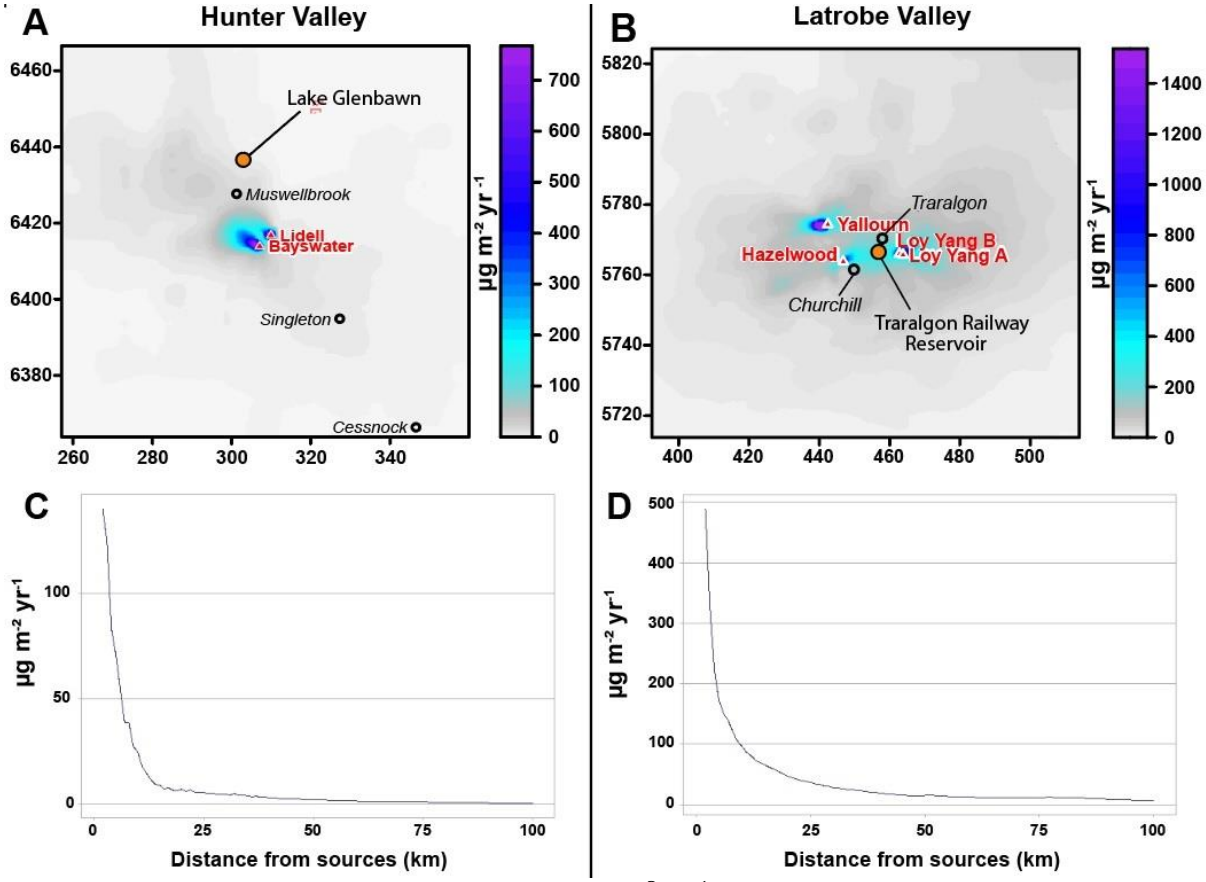

Figure 5 - Annual total mercury deposition (µg m^{-2} yr^{-1}) from coal-fired power plants in the Hunter Valley (New South Wales) and Latrobe Valley (Victoria). The X and Y axis in A and B denotes the Universal Transverse Mercator (UTM) coordinates. Note that C and D deposition rates were calculated starting at 1 km distance from sources, defined for each cell as the distance to the nearest power station.